

Semi-Empirical Calculations of the Transport Properties of Eight Binary Gas Mixtures at Low Density by the Inversion Method: Part II

Mohammad Hadi Ghattee,* Mohammad Mehdi Papari, and Ali Boushehri

Department of Chemistry, Shiraz University, Shiraz 71454, Iran

(Received September 29, 1998)

The viscosities, diffusion coefficients, and thermal diffusion factors for eight binary gas mixtures: He+SF₆, He+CO₂, He+O₂, He+N₂O, CH₄+SF₆, CH₄+CO₂, CH₄+O₂, and CH₄+N₂O were determined from the extended law of corresponding states for viscosity using the inversion technique for the corresponding interaction potential energies. Lennard–Jones (12-6), (LJ (12-6)), potential function is used as the initial model potential required by the technique. The interaction potential energies from this inversion technique reproduce the viscosities within 1%, the diffusion coefficients within 5%, and the thermal diffusion factors within 25%. The interaction potential energy determined from this inversion method for He+SF₆ system is compared with other methods.

The results of statistical-mechanical theory provide theoretical expressions for various equilibrium and non-equilibrium properties of substances in terms of the potential energy of interaction between a pair of molecules.¹⁾ Given the importance of these properties and thus their prediction, it seems reasonable to attempt to produce an accurate pair potential energy.

The direct measurement of the potential energy between molecules is impossible, so the indirect methods play an important role in determination of interaction potential energies. The indirect methods are based on the extraction of information about forces between molecules from the following sources: 1) transport data, 2) equilibrium properties, 3) quantum mechanical calculations, 4) spectroscopic observations, and 5) molecular beam studies.

Jonah and Rowlinson started an indirect method when the temperature virial coefficients of helium were inverted to determine repulsive forces.²⁾ Later a method proposed by Dymond³⁾ has been used to determine the repulsive forces of inert gases directly from viscosity data.⁴⁾ The Dymond method was based on the one that devised by Hirschfelder and Eliason for the calculation of approximate transport properties.⁵⁾

The iterative inversion procedure, which is an extension of Dymond's method, for extraction of the full potential energy curve from equilibrium and transport data was proposed by Smith et al.^{6–8)} This method will be explained in the next two sections. It has been used also to invert the vibrational and rotational fine structures of IR and UV absorption spectra of diatomic molecules,^{9,10)} and to invert the differential cross sections obtained in molecular beam studies to produce the potential function proposed by Buck¹¹⁾ and Siska et al.¹²⁾ Mobility data also have been successfully inverted to obtain ion-neutral potentials directly between alkali ions and rare gas atoms by Viehland et al.¹³⁾ The inversions of transport and

equilibrium data and their corresponding states correlation have been applied by Boushehri et al.^{14–20)}

Our previous work (part I)²¹⁾ was concerned with the direct inversion of the viscosity collision integrals obtained from the extended law of corresponding states to produce pairwise interaction potential energies and the corresponding transport properties of eight equimolar binary gas mixtures (Ar+O₂, Ar+CO₂, Ar+SF₆, Ar+N₂O, Ne+O₂, Ne+CO₂, Ne+SF₆, and Ne+N₂O). In the present paper, this method has been applied to eight other equimolar binary gas mixtures (He+SF₆, He+O₂, He+CO₂, He+N₂O, CH₄+SF₆, CH₄+O₂, CH₄+CO₂, and CH₄+N₂O). Our estimated accuracies are within 1% for viscosities, 5% for binary diffusion coefficients and 25% for thermal diffusion factors.

Kinetic Theory of Gases

For gases at low density, the transport coefficients depend on the binary interactions between molecules in the gas. The Chapman–Enskog solution of the Boltzman kinetic equation for dilute monatomic gases relates these coefficients to a series of collision integrals $\mathcal{Q}^{(l,s)}$. The scattering angle, θ , the transport collision integral, $Q^{(l)}$, and the collision integral, $\mathcal{Q}^{(l,s)}$, are defined as:¹⁾

$$\theta = \pi - 2b \int_{r_0}^{\infty} \frac{r^{-2} dr}{\{1 - (b^2/r^2) - (V(r)/E)\}^{1/2}}, \quad (1)$$

$$Q^{(l)}(E) = 2\pi \left[1 - \frac{1 + (-1)^l}{2(1+l)} \right]^{-1} \int_0^{\infty} (1 - \cos^l \theta) b db, \quad (2)$$

$$\mathcal{Q}^{(l,s)}(T) = \left[(s+1)!(kT)^{s+2} \right]^{-1} \int_0^{\infty} Q^{(l)}(E) \exp(-E/kT) E^{s+1} dE, \quad (3)$$

where b is the impact parameter, r_0 is the closest approach of two trajectories, E is the relative kinetic energy of colliding

partners, and kT has its usual meaning.

Thus three successive numerical integrations are required to obtain a collision integral. The collision integral depends on temperature T , and well depth ε , but it is convenient to express the variables in terms of a dimensionless quantity T^* defined by

$$T^* = kT/\varepsilon. \quad (4)$$

The reduced collision integral, therefore, depends on T^* only.

For the viscosity as a transport property, Eqs. 2 and 3 can be expressed respectively by

$$Q^{(2)} = 3\pi \int_0^\infty [1 - \cos^2 \theta(b, E)] b db, \quad (5)$$

$$\Omega^{(2,2)} = [6(kT)^4]^{-1} \int_0^\infty Q^{(2)}(E) \exp(-E/kT) E^3 dE. \quad (6)$$

The kinetic theory expression for the viscosity coefficient of a pure monatomic dilute gas of molecule mass m at the temperature T is

$$\eta = \frac{5}{16} \frac{(\pi m k T)^{1/2}}{\Omega^{(2,2)}(T)} f_\eta, \quad (7)$$

where f_η represents the higher-order correction to the first kinetic theory approximation. Its value is obtained by:

$$f_\eta = 1 + \frac{3}{196} (8E^* - 7)^2, \quad (8)$$

where E^* is the ratio of collision integrals. (See Eq. 15)

Inversion Scheme. The inversion procedure initiates if an estimated model potential and the well depth, ε , are known. It is encouraging that the ε value can be determined from viscosity data alone.²²⁾ The idea behind this approach is based on considering a reasonable model potential to calculate G , the inversion function, as a function of T^* for converting the experimental data points ($\Omega_{\text{Exp}}^{*(2,2)}, T^*$) to the related pair values (V^*, r^*) on the potential energy curve, using these equations:

$$V^* = V/\varepsilon = GT^*, \quad (9)$$

and

$$r^* = r/\sigma = (\Omega^{*(2,2)})^{1/2}. \quad (10)$$

G values for potentials with a short-range repulsion, a long-range attraction, and a single smooth minimum in the intermediate region, depend almost entirely on the single parameter T^* . The values of G for LJ(12-6) model potential as an initial model have been taken from Viehland et al.'s tabulation.¹³⁾ The reduced viscosity collision integral may be defined as

$$\Omega^{*(2,2)} = \Omega^{(2,2)}/\pi\sigma^2. \quad (11)$$

Here σ is a length scaling factor such that $V(\sigma) = 0$. Since V in our work is defined such that $V(\sigma_0) = 0$, it turns out to that the value of σ is nearly equal to σ_0 : precisely, $\sigma/\sigma_0 = 0.997$.

It must be mentioned that $\Omega_{\text{Exp}}^{*(2,2)}$ values are obtained from the correlation equations given in Ref. 23.

The new potentials obtained by Eqs. 9 and 10 are closer approximations to the true potential than was the initial model

potential. The new potential is used to calculate collision integrals by integrating Eqs. 1, 2, and 3 using the Gatland version of the computer program developed by O'Hara and Smith^{24,25)} and the process is repeated until a convergence occurs. The convergence condition is the degree to which a calculated collision integral around an iteration is in close agreement with the one obtained from corresponding states correlation⁶⁾ and also the degree to which the intermolecular potential energies obtained by inversion, reproduce thermo-physical properties consistent with the experimental values.

The results given in the following section have converged after two iterations.

Results and Discussion

The traditional procedure for extracting of potential energy is represented by introducing a potential energy function with several adjustable parameters. It has the disadvantage that it can not produce a unique potential energy. But the inversion procedure of transport collision integrals, especially the viscosity collision integral presented in this work, is obviously a powerful method for the calculation of unlike molecular interaction potentials. This potential can reproduce transport properties within the experimental accuracy. A major advantage of this approach, therefore, is that the need of a potential function with adjustable parameters is removed and the approach also guarantees a unique potential energy.

It should be mentioned that this paper is concerned with molecular gases rather than just binary noble gases or CH_4 (nearly noble gases) + noble gases, like the previous ones. It comes as somewhat of a surprise that a spherical potential serves for a wide variety of molecular gases (O_2 , N_2O , CO_2 , and SF_6) with sufficient accuracy for our purposes.

In this work, we have obtained accurate reduced potentials for eight binary gas mixtures. In Fig. 1, typically, a reduced pair potential energy curve has been given for $\text{He} + \text{SF}_6$ system and compared with those obtained experimentally by other methods.^{26,27)} We could observe some discrepancies between the potential energy from the inversion procedure, that we have claimed to be reliable, and the potential energy obtained by Kupperman et al.²⁶⁾ and Taylor and Urly.²⁷⁾ These discrepancies are more explicit in the short-range region than in the other regions. It is of important to note that recently it has been shown that Kupperman's potential²⁶⁾ exhibits a discrepancy from that obtained by Chapman et al.²⁸⁾ Taylor's potential has been obtained mainly from thermal diffusion measurements. On the other hand the revision of the extended principle of the corresponding states by Najafi et al.²⁹⁾ and Bzowski et al.²³⁾ correlates properties of the noble gases, molecular gases, and all their mixtures at low density over a very large temperature range with excellent accuracy and characterizes each binary interaction with the aid of five classical material parameters: σ , ε , ρ^* , V_0^* , C_6^* . C_6^* characterizes well the long-range attractive tail of the potential and ρ^* plus V_0^* characterize the short-range repulsive one. Therefore our binary interaction potential is more accurate than those obtained by the other methods.

We have used our reasonably accurate potentials to obtain

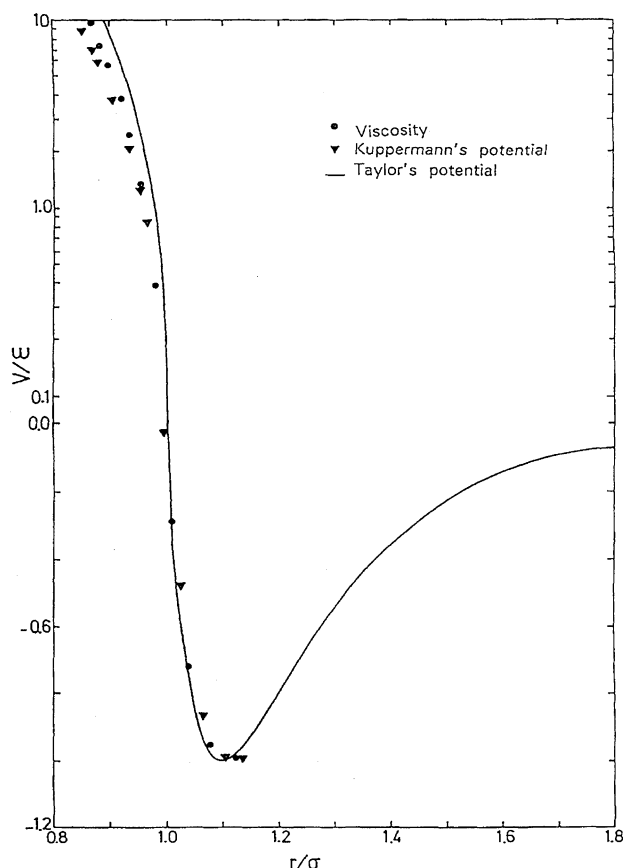


Fig. 1. The reduced pair potential energy for He+SF₆ system. The results of inversion of the viscosity data shown by ●. The solid line (—) shown for comparison, is Taylor's potential. Kupperman's potential is shown by ▼.

the improved kinetic theory collision integrals necessary for the calculation of transport properties. Finally, these collision integrals have been used to calculate viscosities, diffusion coefficients, and thermal diffusion factors as transport properties. Collision integrals in conjunction with their ratios are shown in Tables 1, 2, 3, 4, 5, 6, 7, and 8 for eight binary mixtures. The ratios of the collision integrals have been calculated by the following equations:

$$A^* = \Omega^{*(2,2)} / \Omega^{*(1,1)}, \quad (12)$$

Table 1. The Reduced Collision Integrals and Their Ratios for ⁴He+SF₆ System

log T*	Ω ^{*(1,1)}	Ω ^{*(2,2)}	A*	B*	C*	E*	F*
0.0	1.4000	1.5616	1.1154	1.1955	0.8492	0.8813	0.9229
0.2	1.1541	1.2737	1.1036	1.1448	0.8731	0.9000	0.9389
0.4	0.9874	1.0846	1.0984	1.1135	0.9007	0.9251	0.9612
0.6	0.8747	0.9623	1.1002	1.0978	0.9226	0.9436	0.9826
0.8	0.7945	0.8768	1.1036	1.0894	0.9371	0.9543	0.9984
1.0	0.7332	0.8110	1.1060	1.0848	0.9460	0.9606	1.0078
1.2	0.6830	0.7576	1.1092	1.0856	0.9507	0.9652	1.0123
1.4	0.6388	0.7115	1.1138	1.0859	0.9523	0.9654	1.0174
1.6	0.5990	0.6643	1.1090	1.0694	0.9556	0.9598	1.0253
1.8	0.5667	0.6153	1.0857	1.0378	0.9653	0.9586	1.0282
2.0	0.5454	0.5742	1.0530	1.0105	0.9792	0.9679	1.0230

Table 2. The Reduced Collision Integrals and Their Ratios for ⁴He+O₂ System

log T*	Ω ^{*(1,1)}	Ω ^{*(2,2)}	A*	B*	C*	E*	F*
0.0	1.3977	1.5530	1.1111	1.1955	0.8482	0.8821	0.9222
0.2	1.1512	1.2677	1.1013	1.1437	0.8727	0.9006	0.9385
0.4	0.9848	1.0807	1.0975	1.1131	0.9008	0.9258	0.9608
0.6	0.8723	0.9607	1.1013	1.1007	0.9223	0.9449	0.9817
0.8	0.7912	0.8773	1.1089	1.0975	0.9351	0.9553	0.9972
1.0	0.7268	0.8122	1.1175	1.0995	0.9413	0.9604	1.0069
1.2	0.6711	0.7570	1.1280	1.1073	0.9425	0.9627	1.0121
1.4	0.6190	0.7053	1.1394	1.1123	0.9405	0.9591	1.0187
1.6	0.5702	0.6482	1.1368	1.0929	0.9420	0.9491	1.0286
1.8	0.5298	0.5874	1.1087	1.0520	0.9534	0.9462	1.0321
2.0	0.5028	0.5367	1.0674	1.0152	0.9713	0.9579	1.0261

Table 3. The Reduced Collision Integrals and Their Ratios for ⁴He+CO₂ System

log T*	Ω ^{*(1,1)}	Ω ^{*(2,2)}	A*	B*	C*	E*	F*
0.0	1.3984	1.5606	1.1160	1.1954	0.8490	0.8813	0.9234
0.2	1.1526	1.2726	1.1041	1.1449	0.8730	0.8998	0.9391
0.4	0.9860	1.0833	1.0987	1.1137	0.9006	0.9250	0.9612
0.6	0.8732	0.9614	1.1010	1.0993	0.9223	0.9439	0.9822
0.8	0.7924	0.8766	1.1063	1.0936	0.9360	0.9547	0.9976
1.0	0.7296	0.8113	1.1121	1.0929	0.9435	0.9607	1.0070
1.2	0.6763	0.7574	1.1200	1.0986	0.9460	0.9642	1.0119
1.4	0.6274	0.7085	1.1293	1.1024	0.9452	0.9619	1.0180
1.6	0.5820	0.6555	1.1262	1.0839	0.9473	0.9533	1.0274
1.8	0.5446	0.5989	1.0997	1.0463	0.9581	0.9509	1.0308
2.0	0.5197	0.5517	1.0616	1.0132	0.9745	0.9618	1.0249

Table 4. The Reduced Collision Integrals and Their Ratios for ⁴He+N₂O System

log T*	Ω ^{*(1,1)}	Ω ^{*(2,2)}	A*	B*	C*	E*	F*
0.0	1.4000	1.5551	1.1108	1.1961	0.8483	0.8824	0.9222
0.2	1.1530	1.2703	1.1018	1.1446	0.8726	0.9006	0.9384
0.4	0.9859	1.0825	1.0979	1.1132	0.9005	0.9253	0.9611
0.6	0.8732	0.9610	1.1006	1.0987	0.9224	0.9440	0.9823
0.8	0.7927	0.8764	1.1057	1.0928	0.9363	0.9548	0.9977
1.0	0.7301	0.8113	1.1112	1.0918	0.9439	0.9608	1.0071
1.2	0.6773	0.7577	1.1187	1.0973	0.9466	0.9645	1.0118
1.4	0.6289	0.7094	1.1280	1.1013	0.9559	0.9625	1.0178
1.6	0.5839	0.6571	1.1254	1.0838	0.9478	0.9540	1.0271
1.8	0.5466	0.6011	1.0998	1.0468	0.9582	0.9514	1.0307
2.0	0.5216	0.5539	1.0620	1.0137	0.9744	0.9618	1.0250

Table 5. The Reduced Collision Integrals and Their Ratios for CH₄+SF₆ System

log T*	Ω ^{*(1,1)}	Ω ^{*(2,2)}	A*	B*	C*	E*	F*
0.0	1.4001	1.5606	1.1147	1.1953	0.8487	0.8814	0.9232
0.2	1.1537	1.2733	1.1037	1.14445	0.8729	0.9002	0.9392
0.4	0.9869	1.0843	1.0986	1.1133	0.9007	0.9250	0.9615
0.6	0.8743	0.9620	1.1003	1.0978	0.9227	0.9436	0.9827
0.8	0.7941	0.8765	1.1037	1.0896	0.9371	0.9544	0.9983
1.0	0.7328	0.8109	1.1065	1.0856	0.9458	0.9607	1.0076
1.2	0.6824	0.7576	1.1103	1.0870	0.9502	0.9652	1.0122
1.4	0.6377	0.7113	1.1155	1.0878	0.9515	0.9651	1.0174
1.6	0.5972	0.6636	1.1111	1.0712	0.9546	0.9591	1.0255
1.8	0.5643	0.6137	1.0875	1.0392	0.9645	0.9577	1.0285
2.0	0.5424	0.5718	1.0541	1.0109	0.9786	0.9671	1.0233

Table 6. The Reduced Collision Integrals and Their Ratios for CH₄+O₂ System

log T^*	$\Omega^{*(1,1)}$	$\Omega^{*(2,2)}$	A^*	B^*	C^*	E^*	F^*
0.0	1.4024	1.5621	1.1139	1.1978	0.8481	0.8804	0.9212
0.2	1.1543	1.2720	1.1020	1.1451	0.8720	0.8992	0.9373
0.4	0.9865	1.0823	1.0971	1.1134	0.9002	0.9251	0.9599
0.6	0.8732	0.9613	1.1009	1.1008	0.9219	0.9447	0.9811
0.8	0.7916	0.8778	1.1089	1.0979	0.9348	0.9553	0.9968
1.0	0.7270	0.8126	1.1177	1.0998	0.9410	0.9602	1.0068
1.2	0.6710	0.7570	1.1281	1.1071	0.9424	0.9624	1.0122
1.4	0.6190	0.7050	1.1391	1.1117	0.9406	0.9589	1.0188
1.6	0.5703	0.6479	1.1361	1.0921	0.9423	0.9492	1.0285
1.8	0.5301	0.5873	1.1079	1.0513	0.9537	0.9465	1.0320
2.0	0.5034	0.5370	1.0668	1.0149	0.9716	0.9583	1.0260

Table 7. The Reduced Collision Integrals and Their Ratios for CH₄+CO₂ System

log T^*	$\Omega^{*(1,1)}$	$\Omega^{*(2,2)}$	A^*	B^*	C^*	E^*	F^*
0.0	1.3999	1.5616	1.1156	1.1962	0.8485	0.8807	0.9229
0.2	1.1530	1.2724	1.1035	1.1447	0.8726	0.8995	0.9387
0.4	0.9860	1.0828	1.0982	1.1134	0.9005	0.9250	0.9608
0.6	0.8732	0.9613	1.1009	1.0997	0.9222	0.9442	0.9818
0.8	0.7922	0.8771	1.1071	1.0950	0.9357	0.9550	0.9974
1.0	0.7288	0.8118	1.1139	1.0951	0.9427	0.9605	1.0070
1.2	0.6747	0.7573	1.1225	1.1012	0.9449	0.9636	1.0120
1.4	0.6248	0.7075	1.1323	1.1053	0.9438	0.9611	1.0182
1.6	0.5784	0.6533	1.1295	1.0868	0.9457	0.9521	1.0277
1.8	0.5400	0.5955	1.1028	1.0484	0.9566	0.9495	1.0312
2.0	0.5143	0.5472	1.0638	1.0141	0.9734	0.9605	1.0254

Table 8. The Reduced Collision Integrals and Their Ratios for CH₄+N₂O System

log T^*	$\Omega^{*(1,1)}$	$\Omega^{*(2,2)}$	A^*	B^*	C^*	E^*	F^*
0.0	1.3998	1.5616	1.1156	1.1962	0.8485	0.8808	0.9230
0.2	1.1530	1.2725	1.1036	1.1447	0.8726	0.8996	0.9389
0.4	0.9860	1.0829	1.0983	1.1135	0.9005	0.9250	0.9609
0.6	0.8732	0.9613	1.1009	1.0996	0.9223	0.9442	0.9819
0.8	0.7923	0.8770	1.1070	1.0947	0.9357	0.9550	0.9974
1.0	0.7289	0.8118	1.1137	1.0948	0.9428	0.9606	1.0070
1.2	0.6749	0.7574	1.1222	1.1009	0.9450	0.9637	1.0120
1.4	0.6252	0.7076	1.1320	1.1049	0.9440	0.9612	1.0181
1.6	0.5788	0.6536	1.1291	1.0865	0.9459	0.9523	1.0277
1.8	0.5406	0.5960	1.1025	1.0482	0.9567	0.9497	1.0312
2.0	0.5150	0.5478	1.0636	1.0140	0.9735	0.9607	1.0254

$$B^* = (5\Omega^{*(1,2)} - 4\Omega^{*(1,3)})/\Omega^{*(1,1)}, \quad (13)$$

$$C^* = \Omega^{*(1,2)}/\Omega^{*(1,1)}, \quad (14)$$

$$E^* = \Omega^{*(2,3)}/\Omega^{*(2,2)}, \quad (15)$$

$$F^* = \Omega^{*(3,3)}/\Omega^{*(1,1)}. \quad (16)$$

It must be mentioned that we are concerned only with temperatures related to $T^* \geq 1.0$ because viscosity collision integrals for molecular gases at low temperature are not available (for further discussions see Ref. 30). Therefore, an extrapolation function at low temperatures (long-range region) has been applied which reads as $V^* = -C_6 u^6$, where, C_6 is the

dispersion coefficient and u is the reciprocal of the intermolecular separation, both in atomic units.

The main advantage of the ratios of collision integrals ob-

Table 9. The Predicted Transport Properties of an Equimolar Mixture of ⁴He+SF₆

T	η	D (1.013 bar)	α_T
K	$\mu\text{Pa s}$	$10^{-4} \text{ m}^2 \text{ s}^{-1}$	
273.15	16.24	0.3484	0.4883
313.15	18.21	0.4369	0.4928
353.15	20.09	0.5327	0.4955
423.15	23.24	0.7176	0.4986
473.15	25.33	0.8626	0.5002
523.15	27.39	1.0176	0.5016
573.15	29.31	1.1826	0.5030
623.15	31.20	1.3572	0.5046

Table 10. The Predicted Transport Properties of an Equimolar Mixture ⁴He+O₂

T	η	D (1.013 bar)	α_T
K	$\mu\text{Pa s}$	$10^{-4} \text{ m}^2 \text{ s}^{-1}$	
273.15	20.33	0.6611	0.3726
313.15	22.50	0.8314	0.3756
353.15	24.54	1.0172	0.3778
423.15	27.91	1.3764	0.3788
473.15	30.19	1.6590	0.3788
523.15	32.38	1.9625	0.3783
573.15	34.47	2.2865	0.3775
623.15	36.52	2.6301	0.3765

Table 11. The Predicted Transport Properties of an Equimolar Mixture of ⁴He+CO₂

T	η	D (1.013 bar)	α_T
K	$\mu\text{Pa s}$	$10^{-4} \text{ m}^2 \text{ s}^{-1}$	
273.15	16.55	0.5399	0.3991
313.15	18.54	0.6791	0.4057
353.15	20.43	0.8310	0.4111
423.15	23.60	1.1243	0.4173
473.15	25.76	1.3540	0.4198
523.15	27.81	1.6006	0.4219
573.15	29.84	1.8630	0.4229
623.15	31.73	2.1408	0.4234

Table 12. The Predicted Transport Properties of an Equimolar Mixture ⁴He+N₂O

T	η	D (1.013 bar)	α_T
K	$\mu\text{Pa s}$	$10^{-4} \text{ m}^2 \text{ s}^{-1}$	
273.15	16.62	0.5484	0.3955
313.15	18.61	0.6901	0.4014
353.15	20.55	0.8449	0.4091
423.15	23.80	1.1428	0.4157
473.15	25.96	1.3768	0.4192
523.15	28.09	1.6272	0.4214
573.15	30.11	1.8941	0.4232
623.15	32.07	2.1762	0.4239

tained from inversion of the corresponding states viscosity is that it is more accurate than those obtained from other corresponding states because measurements of viscosity are

Table 13. The Predicted Transport Properties of an Equimolar Mixture of CH₄+SF₆

T	η	D (1.013 bar)	α_T
K	$\mu\text{Pa s}$	$10^{-4} \text{ m}^2 \text{ s}^{-1}$	
273.15	13.76	0.0970	0.1533
313.15	15.56	0.1253	0.1820
353.15	17.27	0.1564	0.2062
423.15	20.12	0.2176	0.2409
523.15	23.86	0.3184	0.2768
623.15	27.27	0.4333	0.3019
773.15	31.98	0.6303	0.3274
973.15	37.68	0.9352	0.3491
1173.15	42.89	1.2838	0.3631
1773.15	56.68	2.5660	0.3856
2273.15	66.75	3.8760	0.3943
2773.15	75.95	5.3846	0.3990
3273.15	84.50	7.0791	0.4016

Table 14. The Predicted Transport Properties of an Equimolar Mixtures of CH₄+O₂

T	η	D (1.013 bar)	α_T
K	$\mu\text{Pa s}$	$10^{-4} \text{ m}^2 \text{ s}^{-1}$	
273.15	14.78	0.1928	0.0754
313.15	16.56	0.2474	0.0873
353.15	18.25	0.3079	0.0972
423.15	21.02	0.4255	0.1109
523.15	24.62	0.6178	0.1241
623.15	27.91	0.8368	0.1327
773.15	32.44	1.2118	0.1409
973.15	37.94	1.7918	0.1471
1173.15	43.01	2.4568	0.1506
1773.15	56.53	4.9141	0.1542
2273.15	66.58	7.4459	0.1539
2773.15	75.40	10.3864	0.1529
3273.15	84.76	13.7118	0.1517

Table 15. The Predicted Transport Properties of an Equimolar Mixture of CH₄+CO₂

T	η	D (1.013 bar)	α_T
K	$\mu\text{Pa s}$	$10^{-4} \text{ m}^2 \text{ s}^{-1}$	
273.15	12.54	0.1449	0.0691
313.15	14.25	0.1882	0.0863
353.15	15.84	0.2355	0.1024
423.15	18.54	0.3293	0.1258
523.15	22.09	0.4845	0.1512
623.15	25.36	0.6628	0.1697
773.15	29.83	0.9682	0.1884
973.15	35.21	1.4421	0.2040
1173.15	40.11	1.9850	0.2135
1773.15	53.11	3.9902	0.2278
2273.15	62.67	6.0491	0.2326
2773.15	71.44	8.4291	0.2347
3273.15	79.64	11.1115	0.2351

much more accurate than measurements of the other properties (say, diffusion). Besides, rather limited experimental data on transport properties except viscosity are available because, in general, the measurement of viscosity is more

Table 16. The Predicted Transport Properties of an Equimolar Mixture of CH₄+N₂O

T	η	D (1.013 bar)	α_T
K	$\mu\text{Pa s}$	$10^{-4} \text{ m}^2 \text{ s}^{-1}$	
273.15	12.52	0.1449	0.0632
313.15	14.22	0.1881	0.0805
353.15	15.85	0.2359	0.0960
423.15	18.60	0.3306	0.1197
523.15	22.21	0.4873	0.1457
623.15	25.50	0.6662	0.1642
773.15	30.05	0.9748	0.1837
973.15	35.54	1.4538	0.2000
1173.15	40.55	2.0032	0.2103
1773.15	53.80	4.0321	0.2256
2273.15	63.51	6.1144	0.2309
2773.15	72.43	8.5217	0.2334
3273.15	80.75	11.2340	0.2344

Table 17. Deviation of the Calculated Values of the Diffusion Coefficients of Mixtures From the Experimental Values

He+O ₂ ^{a)}							
T (K)	195.10	205.20	218.07	234.22	255.50	280.00	290.00
D_{Expt}	0.3644	0.3957	0.4378	0.4934	0.5710	0.6624	0.7032
D_{Calcd}	0.3696	0.4026	0.4464	0.5036	0.5830	0.6804	0.7215
Dev% ^{b)}	-1.41	-1.71	-1.93	-2.03	-2.06	-2.65	-2.54
T (K)	300.00	320.00	337.90	356.07	373.09	385.49	400.21
D_{Expt}	0.7448	0.8305	0.9104	0.9939	1.072	1.135	1.208
D_{Calcd}	0.7636	0.8508	0.9323	1.0179	1.1004	1.1623	1.2374
Dev% ^{b)}	-2.46	-2.39	-2.35	-2.36	-2.58	-2.35	-2.38
He+CO ₂ ^{a)}							
T (K)	195.10	205.20	218.07	234.22	255.50	280.00	290.00
D_{Expt}	0.2927	0.3188	0.3539	0.3991	0.4620	0.5366	0.5689
D_{Calcd}	0.3007	0.3279	0.3638	0.4106	0.4758	0.5553	0.5891
Dev% ^{b)}	-2.66	-2.78	-2.72	-2.80	-2.90	-3.37	-3.43
T (K)	300.00	320.00	337.90	356.07	373.09	385.49	400.21
D_{Expt}	0.6023	0.6704	0.7362	—	0.8708	0.9179	0.9780
D_{Calcd}	0.6236	0.6950	0.7617	0.8314	0.8989	0.9493	1.0108
Dev% ^{b)}	-3.42	-3.54	-3.35	—	-3.12	-3.42	-3.25
He+SF ₆ ^{a)}							
T (K)	195.10	205.20	218.07	234.22	255.50	280.00	290.00
D_{Expt}	0.1899	0.2057	0.2284	0.2585	—	0.3469	0.3680
D_{Calcd}	0.1966	0.2138	0.2366	0.2665	0.3079	0.3583	0.3797
Dev% ^{b)}	-3.41	-3.79	-3.47	-3.00	—	-3.18	-3.08
T (K)	300.00	320.00	337.90	356.07	373.09	385.49	400.21
D_{Expt}	0.3894	0.4332	0.4758	0.5190	0.5593	0.5912	0.6281
D_{Calcd}	0.4017	0.4468	0.4888	0.5328	0.5756	0.6074	0.6461
Dev% ^{b)}	-3.06	-3.04	-2.66	-2.59	-2.83	-2.67	-2.79

a) Ref. 31. b) Dev% = $\frac{D_{\text{Exp}} - D_{\text{Calcd}}}{D_{\text{Calcd}}} \times 100$.

Table 18. Deviation of the Calculated Values of the Thermal Diffusion Factors of Mixtures From the Experimental Values

$T = 255.3 \text{ K}$					
He+SF ₆ ^{a)}					
X_{SF_6}	0.189	0.199	0.788	0.806	
$(\alpha_T)_{\text{Expt}}$	0.8099	0.7976	0.3690	0.3512	
$(\alpha_T)_{\text{Calcd}}$	0.8552	0.8348	0.3473	0.3412	
Dev% ^{b)}	-5.30	-4.46	6.25	2.93	
$T = 300.0 \text{ K}$					
X_{SF_6}	0.200	0.788	0.809		
$(\alpha_T)_{\text{Expt}}$	0.8300	0.3701	0.3628		
$(\alpha_T)_{\text{Calcd}}$	0.8427	0.3515	0.3443		
Dev% ^{b)}	-1.50	5.29	5.37		
$T = 255.3 \text{ K}$					
He+CO ₂ ^{c)}					
X_{CO_2}	0.190	0.199	0.210	0.790	0.810
$(\alpha_T)_{\text{Expt}}$	0.5784	0.5688	0.5807	0.3092	0.3095
$(\alpha_T)_{\text{Calcd}}$	0.5948	0.5861	0.5759	0.3006	0.2957
Dev% ^{b)}	-2.76	-2.95	0.83	2.86	4.67
$T = 255.3 \text{ K}$					
He+O ₂ ^{c)}					
X_{O_2}	0.189	0.209	0.789	0.810	
$(\alpha_T)_{\text{Expt}}$	0.4980	0.4819	0.2931	0.2981	
$(\alpha_T)_{\text{Calcd}}$	0.5152	0.5025	0.2941	0.2898	
Dev% ^{b)}	-3.34	-4.10	-0.34	2.86	

a) Ref. 32. b) $\text{Dev\%} = \frac{(\alpha_T)_{\text{Expt}} - (\alpha_T)_{\text{Calcd}}}{(\alpha_T)_{\text{Calcd}}} \times 100$. c) Ref. 31.

practical than those of other transport properties.

Tables 9, 10, 11, 12, 13, 14, 15, and 16 contain predicted viscosities, diffusion coefficients, and thermal diffusion factors of the low density and equimolar binary gas mixtures from inversion method calculated by using the relationships given in Ref. 23. The higher order correction term for viscosity f_η and the higher order correction factor for diffusion Δ_{ij} , have been taken into account. The literature and the calculated values of the diffusion coefficients and the thermal diffusion factors have been given in Tables 17 and 18. Deviations of the calculated from the experimental values have also been included.

Conclusion

The direct inversion technique represents a distinct advance over the traditional methods of force fitting data to potential functions of primitive forms. This scheme provides an accurate potential energy and allows determination of collision integrals more accurately than is possible by the extended law of corresponding states. The accurate potential energy obtained by inversion of viscosity data can reproduce (within the precision of the experimental data) all transport properties.

Our estimated accuracies are within 1% for η (viscosity), 5% for D_{12} (binary diffusion coefficient), and 25% for α_T (thermal diffusion factor) for all eight mixtures.

The authors wish to thank the Computer Center and the Department of Chemistry of Shiraz University for the computer facilities. The authors are also indebted to the Research

Committee of Shiraz University.

References

- 1) J. O. Hirschfelder, C. F. Curtiss, and R. B. Bird, "Molecular Theory of Gases and Liquids," John Wiley, New York (1954), p. 514.
- 2) D. A. Jonah and J. S. Rowlinson, *Trans. Faraday Soc.*, **62**, 1067 (1966).
- 3) J. H. Dymond, *J. Chem. Phys.*, **49**, 3673 (1968).
- 4) H. S. Hahn and E. A. Mason, *Chem. Phys. Lett.*, **9**, 633 (1971).
- 5) J. O. Hirschfelder and M. A. Eliason, *Ann. N.Y. Acad. Sci.*, **67**, 451 (1957).
- 6) D. W. Gough, G. C. Maitland, and E. B. Smith, *Mol. Phys.*, **24**, 151 (1972).
- 7) G. C. Maitland and E. B. Smith, *Mol. Phys.*, **24**, 1185 (1972).
- 8) G. C. Maitland and E. B. Smith, *Chem. Soc. Rev.*, **2**, 181 (1973).
- 9) G. C. Maitland, *Mol. Phys.*, **26**, 513 (1973).
- 10) G. C. Maitland and E. B. Smith, *Mol. Phys.*, **22**, 861 (1971).
- 11) U. Buck, *J. Chem. Phys.*, **54**, 1923 (1971).
- 12) P. Siska, J. M. Parson, T. P. Schafer, F. P. Tully, W. C. Wang, and Y. T. Lee, *Phys. Rev. Lett.*, **25**, 271 (1970).
- 13) L. A. Viehland, E. A. Mason, W. F. Morrison, and M. R. Flannery, *At. Data Nucl. Data Tables*, **16**, 495 (1975).
- 14) A. Boushehri, *Physica*, **97A**, 206 (1979).
- 15) A. Boushehri and J. M. Absardi, *Bull. Chem. Soc. Jpn.*, **62**, 1313 (1989).
- 16) A. Boushehri and A. Maghari, *J. Phys. Soc. Jpn.*, **59**, 4302 (1990).
- 17) E. K. Goharshadi and A. Boushehri, *Bull. Chem. Soc. Jpn.*, **67**, 2403 (1994).
- 18) A. Boushehri and M. H. Mousazadeh, *J. Phys. Soc. Jpn.*, **64**, 331 (1995).
- 19) A. Boushehri and F. S. Hashemi, *Bull. Chem. Soc. Jpn.*, **69**, 67 (1996).
- 20) M. H. Ghatee, M. M. Papari, and A. Boushehri, *Bull. Chem. Soc. Jpn.*, **70**, 2643 (1997).
- 21) M. M. Papari and A. Boushehri, *Bull. Chem. Soc. Jpn.*, **71**, 2757 (1998).
- 22) A. Boushehri, L. A. Viehland, and E. A. Mason, *Chem. Phys.*, **28**, 313 (1978).
- 23) J. Bzowski, J. Kestin, E. A. Mason, and F. J. Uribe, *J. Phys. Chem. Ref. Data*, **19**, 1179 (1990).
- 24) H. O'Hara and F. J. Smith, *J. Comput. Phys.*, **5**, 328 (1970).
- 25) H. O'Hara and F. J. Smith, *Comput. Phys. Commun.*, **2**, 47 (1971).
- 26) J. T. Slankas, M. Koil, and A. Kupperman, *J. Chem. Phys.*, **70**, 1482 (1979).
- 27) W. L. Taylor and J. H. Urly, *J. Chem. Phys.*, **98**, 2291 (1993).
- 28) W. B. Chapman, A. Schiffman, J. M. Hutson, and D. J. Nesbitt, *J. Chem. Phys.*, **105**, 3497 (1996).
- 29) B. Najafi, E. A. Mason, and J. Kestin, *Physica*, **119A**, 387 (1983).
- 30) A. Boushehri, J. Bzowski, J. Kestin, and E. A. Mason, *J. Phys. Chem. Ref. Data*, **16**, 445 (1987).
- 31) R. D. Trengove, K. R. Harris, H. L. Robjohns, and P. J. Dunlop, *Physica*, **131A**, 506 (1985).
- 32) R. D. Trengove, H. L. Robjohns, and P. J. Dunlop, *Physica*, **128A**, 486 (1984).